Quarterly Technical Progress Report
Report Number 15323R12
(October 1, 2005 – December 31, 2005)

DEVELOPMENT AND OPTIMIZATION OF GAS-ASSISTED GRAVITY DRAINAGE (GAGD) PROCESS FOR IMPROVED LIGHT OIL RECOVERY

Work Performed Under Cooperative Agreement
DE-FC26-02NT15323

By

Dandina N. Rao, Ph. D., P. Eng.
(Principal Investigator)

Subhash C. Ayirala, Ph.D.
Madhav M. Kulkarni, Ph.D.
(Research Associates)

Thaer N. N. Mahmoud, (M.S.)
Wagirin Ruiz Paidin, (M.S.)
(Graduate Research Assistants)

The Craft & Hawkins Department of Petroleum Engineering
Louisiana State University and Agricultural & Mechanical College
Baton Rouge, LA 70803

January 2006

Prepared for
United States Department of Energy
National Energy Technology Laboratory

DISCLAIMER

Abstract

This report describes the progress of the project "Development And Optimization of Gas-Assisted Gravity Drainage (GAGD) Process for Improved Light Oil Recovery" for the duration of the thirteenth project quarter (Oct 1, 2005 to Dec 30, 2005). There are three main tasks in this research project. Task 1 is a scaled physical model study of the GAGD process. Task 2 is further development of a vanishing interfacial tension (VIT) technique for miscibility determination. Task 3 is determination of multiphase displacement characteristics in reservoir rocks.

Section I reports experimental work designed to investigate wettability effects of porous medium, on secondary and tertiary mode GAGD performance. The experiments showed a significant improvement of oil recovery in the oil-wet experiments versus the water-wet runs, both in secondary as well as tertiary mode. When comparing experiments conducted in secondary mode to those run in tertiary mode an improvement in oil recovery was also evident. Additionally, this section summarizes progress made with regard to the scaled physical model construction and experimentation. The purpose of building a scaled physical model, which attempts to include various multiphase mechanics and fluid dynamic parameters operational in the field scale, was to incorporate visual verification of the gas front for viscous instabilities, capillary fingering, and stable displacement. Preliminary experimentation suggested that construction of the 2-D model from sintered glass beads was a feasible alternative. During this reporting quarter, several sintered glass mini-models were prepared and some preliminary experiments designed to visualize gas bubble development were completed.

In Section II, the gas-oil interfacial tensions measured in decane-CO_2 system at 100^{o}F and live decane consisting of 25 mole% methane, 30 mole% n-butane and 45 mole% n-decane against CO_2 gas at 160^{o}F have been modeled using the Parachor and newly proposed mechanistic Parachor models. In the decane-CO_2 binary system, Parachor model was found to be sufficient for interfacial tension calculations. The predicted miscibility from the Parachor model deviated only by about 2.5% from the measured VIT miscibility. However, in multicomponent live decane-CO_2 system, the performance of the Parachor model was poor, while good match of interfacial tension predictions has been obtained experimentally using the proposed mechanistic Parachor model. The predicted miscibility from the mechanistic Parachor model accurately matched with the measured VIT miscibility in live decane-CO_2 system, which indicates the suitability of this model to predict miscibility in complex multicomponent hydrocarbon systems.

In the previous reports to the DOE (15323R07, Oct 2004; 15323R08, Jan 2005; 15323R09, Apr 2005; 15323R10, July 2005 and 154323, Oct 2005), the 1-D experimental results from dimensionally scaled GAGD and WAG corefloods were reported for Section III. Additionally, since Section I reports the experimental results from 2-D physical model experiments; this section attempts to extend this 2-D GAGD study to 3-D (4-phase) flow through porous media and evaluate the performance of these processes using reservoir simulation.

Section IV includes the technology transfer efforts undertaken during the quarter. This research work resulted in one international paper presentation in Tulsa, OK; one journal publication; three pending abstracts for SCA 2006 Annual Conference and an invitation to present at the Independents' Day session at the IOR Symposium 2006.

Table of Contents

1. Design and Development of a Scaled Physical Experimental GAGD Model

1.1 Experimental Investigation of the Effect of Bead Pack Wettability on Immiscible GAGD Performance

During this reporting period (September 30, 2004 up to December 31, 2005) the Gas-Assisted Gravity Drainage (GAGD) experiments in a 2-D physical model packed with oil-wet porous media were continued. This further experimentation was designed as an extension of the water-wet 2-Dimensional Hele-Shaw GAGD experiments of Sharma (2005) and was aimed at the investigation of the effects of reservoir wettability (namely, oil wet porous media) on secondary GAGD process performance.

1.1.1 Procedure for Wettability Alteration of the Glass Beads

Since the focus of this experimentation was to evaluate the performance of the GAGD process in oil-wet media, alteration of the wettability of glass beads from water-wet to oil-wet was essential for comparison on a similar basis. The wettability of the glass beads was altered using an organosilane [$(CH_3)Cl_2Si$], and the steps involved were:

1. Glass beads were prepared for the silylation process by initially rinsing with methylene chloride (CH_2Cl_2).
2. The glass beads were then soaked in a 5% solution of di-methyl di-chloro silane ($(CH_3)_2Cl_2Si$) for about 10 minutes (note: caution should be exercised when pouring off the supernatant liquid from the reaction vessel because of anhydrous hydrochloric acid formation).
3. The glass beads were then rinsed with methylene chloride and then finally soaked in methanol (CH_3OH) for about 10 minutes. The excess methanol was poured off and the glass beads were dried in an oven at 200 ^oF for at least 4 hours before being used in the experiments.

The above procedure is well known and is widely used in the literature to alter the wettability of sands from water-wet to oil-wet (Takach et al., 1989).

1.1.2 Experimental Update

A total of four oil-wet 2-D GAGD experiments were conducted during the reporting period, all of which were run in the secondary mode. The experimental results have been summarized in Tables 1.1 and 1.2:

1. CP-S-OW-13-3: Constant pressure (4 psig), secondary mode, oil-wet glass beads with an average diameter of 0.13 mm. Gas: N_2.
2. CP-S-OW-15-2: Constant pressure (4 psig), secondary mode, oil-wet glass beads with an average diameter of 0.15 mm. Gas: N_2.

3. CP-S-OW-60-1: Constant pressure (4 psig), secondary mode, oil-wet glass beads with an average diameter of 0.60 mm. Gas: N_2.
4. CF-S-OW-13-3: Constant mass flow rate (300 cc/min), secondary mode, oil-wet glass beads with an average diameter of 0.13 mm. Gas: N_2.

These various diameters of the glass beads were chosen to obtain desired values of the Bond number ranges for the experiments conducted.

1.1.3 Effect of Wettability of the Porous Medium on GAGD Performance

The change in wettability from water-wet to oil-wet appears to significantly improve the oil recovery, as can be seen from Figures 1.2-a and 1.2-b. The average incremental production can be summarized as follows:

- Constant pressure secondary runs; 0.13 mm : + 7.3 %.
- Constant pressure secondary runs; 0.15 mm : + 10.9 %.
- Constant rate secondary runs; 0.13 mm : + 21.4 %.

The high oil recoveries obtained in oil-wet systems when compared to water-wet systems in this study agree well with the field observations where oil recoveries due to gas injection are higher in oil-wet reservoirs. The displacement of fluids in these experiments is almost piston like because of appreciable gravity segregation effects. Therefore, the length of the two-phase (gas-oil) flow region is negligibly small to enable the application of diffuse flow theories and/or the use of relative permeabilities.

1.1.4 Future Work

Experiments to quantify the degree of the wettability alteration of the glass beads by the silanization process have been planned for the next quarter.

References

1. Sharma, A.P., “Physical Model Experiments of the Gas-Assisted Gravity Drainage Process”, M.S. Thesis, LSU - Petroleum Engineering, August 2005.
2. Takach, N.E., Bennett, L.B., Douglas, C.B., Andersen, M.A. and Thomas, D.C., "Generation of Oil-Wet Model Sandstone Surfaces", SPE Paper 18465 presented at the SPE International Symposium on Oil Field Chemistry, Houston, TX, February 8-10, 1989.

Table 1.1: Model Parameters for the Oil-Wet Runs in Secondary Mode

Model Parameters	CP-S-OW-13-3	CP-S-OW-15-2	CP-S-OW-60-1	CF-S-OW-13-3
Gas	N_2	N_2	N_2	N_2
P (psig)	4	4	4	N/A
Rate (cc/min)	N/A	N/A	N/A	300
D_g(mm)	0.13	0.15	0.60	0.13
INITIAL CONDITIONS				
Pore Volume (cc)	571.5	504.0	516.0	529
Oil Flood Water (cc)	475.5	455.5	433.7	430.5
OOIP (cc)	475.5	455.5	433.7	430.5
Porosity ϕ (%)	39.6	34.9	35.7	36.6
S_{wc} (%)	16.8	9.6	15.9	18.6
S_{oi} (%)	83.2	90.4	84.1	81.4
GAS INJECTION				
k (Darcy)	7.3	5.3	0.8	4.8
N_B	9.1E-06	7.5E-06	6.0E-06	6.9E-06
N_C	5.3E-06	5.7E-07	6.3E-07	1.9E-05
N_G	17.0	15.8	9.6	0.4
Recovery (% OOIP)	74.0	83.6	81.6	81.5

Table 1.2: Model Parameters for the Water-Wet Runs in Secondary Mode

Model Parameters	CP-S-WW-13-1	CF-S-WW-13-1	CP-S-WW-15-1
Gas	N_2	N_2	N_2
P (psig)	4	N/A	4
Rate (cc/min)	N/A	300	N/A
D_g(mm)	0.13	0.13	0.15
INITIAL CONDITIONS			
Pore Volume (cc)	524	528	558
Oil Flood Water (cc)	362.8	362.8	372.8
OOIP (cc)	362.8	362.8	372.8
Porosity ϕ (%)	36.5	36.5	38.6
S_{wc} (%)	30.8	31.3	33.2
S_{oi} (%)	69.2	68.7	66.8
GAS INJECTION			
k (Darcy)	4.7	4.9	8.1
Recovery (% OOIP)	66.7	60.1	72.7

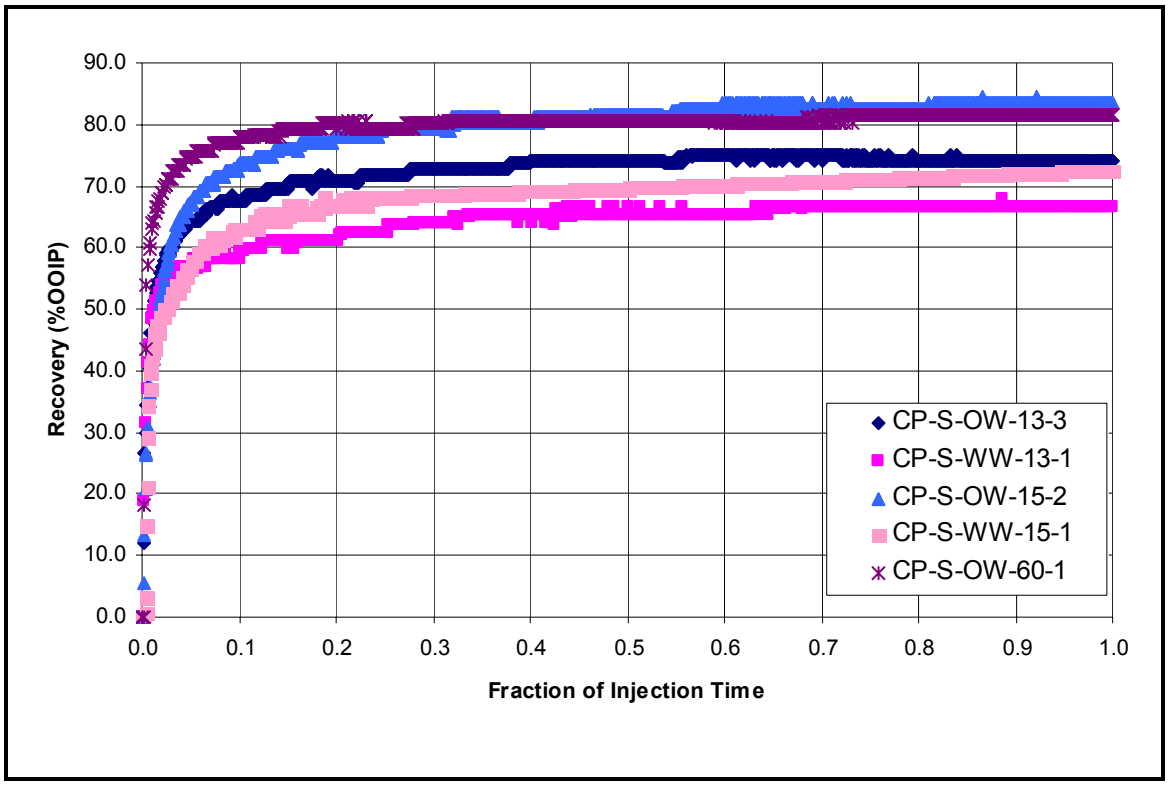

Figure 1.1-a: Oil Recovery vs. Wettability in Constant Pressure Runs

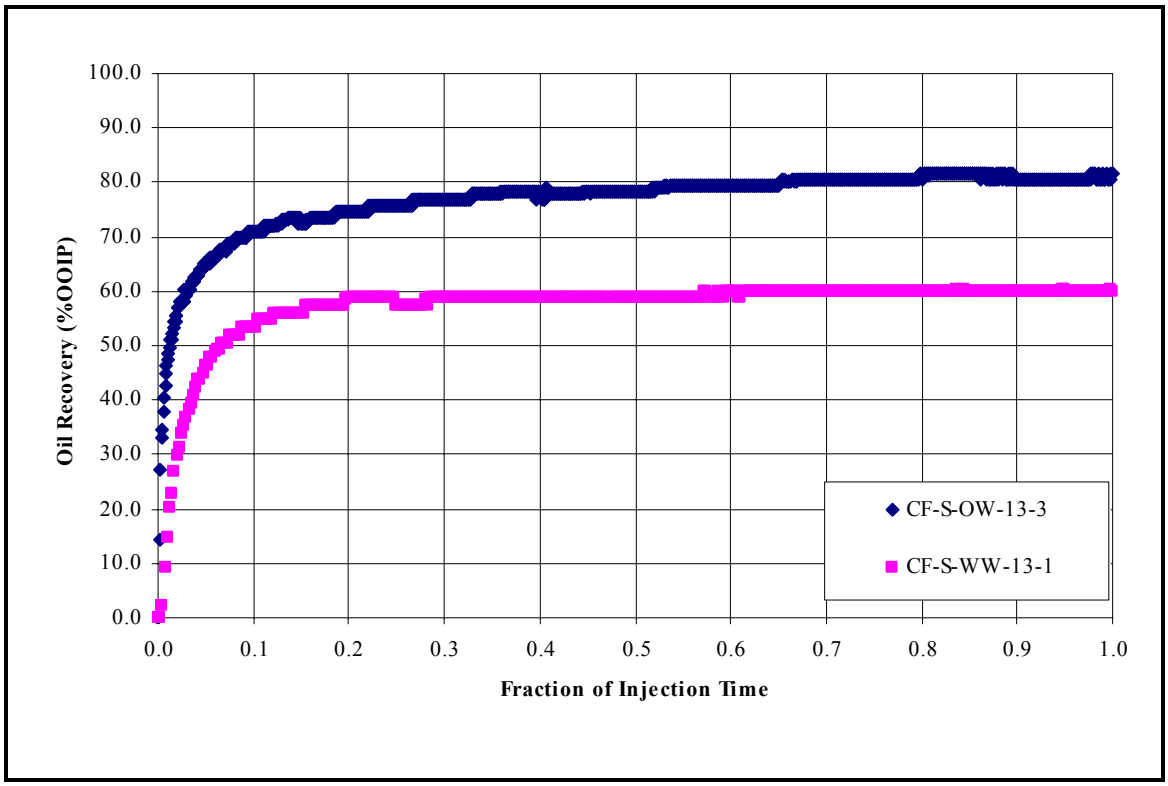

Figure 1.1-b: Oil Recovery vs. Wettability in Constant Rate Runs

1.2 Scaled Model Construction

Preliminary experimentation suggested that construction of the 2-D model from sintered glass beads was a feasible alternative. To facilitate faster and precise experimental controls during model preparation, a high temperature furnace was ordered. The furnace is currently employed to construct, sinter, and test multiple glass models for permeability and porosity.

The preliminary experimentation was started with mini-models (6”X 6”) instead of a full-scale model, since mini models permit the construction and testing at relatively lower costs. These mini-models will also allow us to find the optimum conditions and to obtain the required permeability to simulate the field conditions.

1.2.1 Model Construction

In order to prepare the model for sintering, glass plates were required to be cut to specific sizes. The mini-model a quarter inch thick glass with plates of six inches by six inches, 3/8” inch spacers of the same glass thickness were glued to the glass plates to create the glass bead volume chamber. However, the least amount of glue should be used for this purpose; once the model is sintered, most of the glue (if not all) would evaporate. The excess glue fumes could create a coating around the glass beads possibly, and thereby converting them from water wet to oil wet.

The next step in constructing the mini-model was to fill the model with glass beads of uniform or varying grain dimensions. However, the sharp edges of the glass plates resulted in some leaky areas in the model especially where two glass plates were joined perpendicular to each other. Some silicone sealant was added at the joints to prevent any leaks from the glass bead pack that has yet to be adhered to each other (by sintering). The temporary sealant was found to evaporate away after the sintering. Next, steel end caps were inserted in the model to hold the glass beads in place in the mini-model while it was filled with the glass beads, and made sure that the mini-model was not leaking glass beads. The following protocol was devised to sinter the mini-model at the chosen temperature with selected time length.

After the sintering time the furnace exhaust was opened, and nitrogen was injected at low flow rate in the furnace to circulate the hot air out (cool the furnace down), as well as to stop the sintering process. The objective of N_2 injection was to lower the temperature inside the furnace at fast as possible (without opening the furnace), or induce a thermal shock to the mini-model or the ceramic frame inside the furnace. After the furnace temperature cooled down enough to open (usually under 100^oC), the mini-model was removed, and allowed to complete cooling in the ambient environment. At a later time, the steel end caps were removed and replaced by a 2” plastic (1/4”) line to serve as end caps. The plastic end caps were used instead of steel end caps, because plastic end caps could absorb vibrations that were introduced during the testing phase better than steel end

caps. The plastic end caps were attached to the mini-model using high strength epoxy glue.

The last step before testing the mini-model was to seal the mini-model, which was found to take many trials. Different kind of sealants such as caulking sealants, and automotive sealants were attempted. So far, the most appropriate sealant was found to be a silicone based automotive one (Permatex 66B ®). This sealant was found to cure and gain strength fast (usually within two hours). It may require multiple coats of the sealant to the mini-model to create an effective seal. If the mini-model does not pass the vacuum seal test, gas usually injected at low pressure (2-3 psig), followed by a soapy fluid called Snoop® is sprayed around the sealant to detect the leaks, then the leaks are sealed. The process of sealing is continued until the mini-model passes the vacuum test.

After the leak test, the mini-model porosity was measured by injecting distilled water in a gravity stable manner through the gravity feed system using burettes and 1/8" lines. It is crucial to measure the exact amount of water injected in the mini-model by the lines. Another critical issue for the porosity measurement is calculating the lines' volume (dead volume). This dead volume needs to be deducted from the total volume of water injected. Finally, the porosity of the model is calculated by dividing the net water volume injected by bulk volume of the mini-model.

After the measurement of the mini-model's porosity, the following steps are employed to test the mini-model absolute permeability. This measurement is conducted by injecting distilled water and into the model via the hydrostatic head from the burette to force the distilled water through the sintered glass bead pack. The distilled water is allowed to circulate inside the model to clean and stabilize the glass beads. After a water injection of two to three pore volumes, the mini-model is completely shut. Then, the mini-model is opened to the water gravity feed line and injected water volume and time are measured to calculate the flow rate. It is important not to allow the water level in the burette to be lowered by more than one or two inches, especially if the level of the gravity feed system is not very high. The top of the water in the burette that has been used in the testing the mini-models is set to be equal to 64 inches above the top of the glass beads. If the water level in the burette drops by a higher value, the hydrostatic pressure will greatly vary between the beginning and the end of the test. In the permeability testing, 10 cc liquid is usually used, which is an equivalent to a half inch height in the burette for high accuracy. Finally, Darcy's law is used to calculate the permeability.

1.2.2 Results

To achieve the required permeability, seven models have been constructed and sintered so far with varying one of three variables at a time, namely glass bead size, sintering temperature, and sintering time. Interestingly, permeability testing has suggested that there is an inverse direct relationship between sintering temperature and permeability

values. The relationship suggests that the higher the sintering temperature, the lower the permeability value would be. Also, sintering time has been found to have an inverse direct relationship with the models' permeability (Table 1.3). Ongoing experiments may shed more light in future in establishing more accurate porosity-permeability relationships. The permeabilities of various glass bead models after sintering in this study turned out to be in the range of 501-3034 md. These permeability values are only the results of multiple sintering trails and the optimum one matching the real reservoir permeabilities may be used in future experimentation.

1.2.3 Experimentation

One of the sintered mini-models has been flooded with a red dyed n-decane to evaluate the visual capabilities of the model. The mini-model had an initial oil saturation of 80%, and then it was injected with CO_2, as the primary recovery method. The carbon dioxide did not break through until approximately 70% of the oil was recovered due to the stable flood front (Figure 1.2). It has been observed that if the inlet and outlet of the mini-model is shut in, the oil segregates under the effect of gravity, and accumulates at the lower portion of the mini-model. Moreover, in the upper region of the mini-model, where the carbon dioxide is residing, it appears that the n-decane was completely drained from the upper portion of the mini-model (Figure 1.2). Furthermore, if more carbon dioxide gas was injected, more oil would flow to the outlet from the bottom accumulated oil zone in contrast to conventional continuous gas injection. The CO_2 flood front appeared to be stable under 1-2 psig injection pressure. However, it was observed that the gas cap had a near horizontal flood front, unlike the expected shape of semi circular shape appears to be due to high permeability (1800 mD).

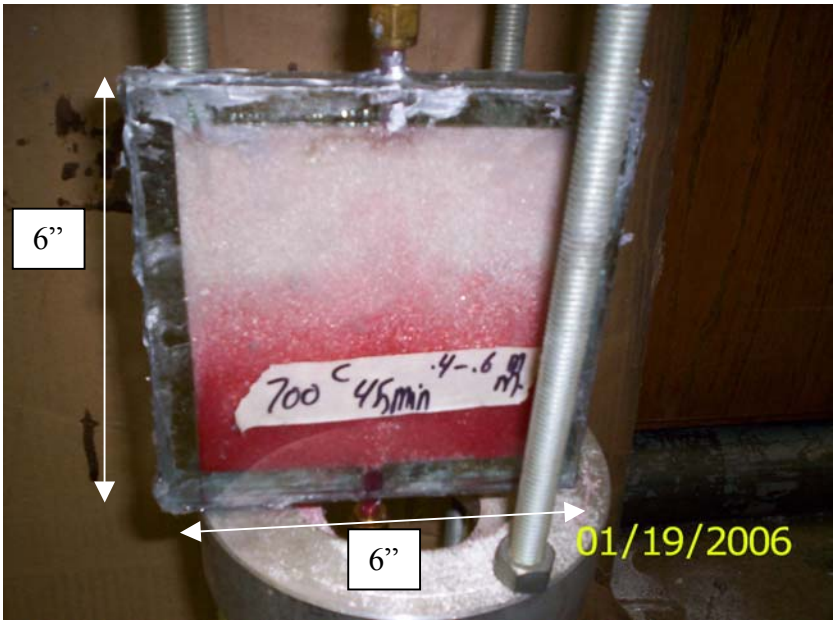

Figure 1.2: A picture of a mini-model that has been sintered, then flooded with water, n-decane, and finally with carbon dioxide. The gravity effect is observed here.

Table 1.3: Table of sintering trials summarizing the conditions (glass bead size, temperature and sintering time) and results (porosity and permeability)

K (mD)	Porosity (%)	Temp (^{o}C)	Time (min)	Glass Bead Size (mm)
1705	21	unknown	unknown	0.1-0.3
990	15	700	45	0.1-0.3
2890	19.7	690	45	0.1-0.3
1800	9.5	700	45	0.4-0.6
3034	22.8	700	30	0.1-0.3
710	5.5	710	45	0.1-0.3
501	6	700	75	0.1-0.3

2. Further Development of the Vanishing Interfacial Tension (VIT) Technique

In the last technical progress report (Report #15323R11, Oct. 2005), under this section, the results of interfacial tension measurements conducted in the two standard gas-oil systems of n-decane-CO_2 at 100^oF and live decane consisting of 25 mole% methane, 30 mole% n-butane and 45 mole% n-decane against CO_2 gas at 160^oF were discussed. The close agreement of miscibilties obtained from the VIT technique in these two standard gas-oil systems with the reported miscibilities from other conventional techniques (rising-bubble and slim-tube) clearly validated the VIT technique to determine miscibility in gas-oil systems. The study of gas-oil ratio effects on interfacial tension indicated that as the fluid phases approach equilibrium, interfacial tension becomes independent of gas-oil ratio, which implies compositional independence of miscibilities determined from the VIT technique. In addition, the dynamic behavior of interfacial tension in gas-oil systems has been identified and reported for the first time using the live decane-CO_2 standard gas-oil system. This report summarizes the modeling of gas-oil interfacial tensions measured in the two standard gas oil systems, using the newly proposed mechanistic Parachor Model. The more details on the proposed mechanistic Parachor model can be found in the previous technical progress report, Report #15323R07, Oct. 2004.

2.1 Modeling of Gas-Oil Interfacial Tension

The interfacial tension measurements in the two standard gas-oil systems of n-decane-CO_2 and live decane-CO_2 at elevated pressures and temperatures reported in the last technical progress report (Report #15323R11, Oct. 2005) were modeled using the Parachor and newly proposed mechanistic Parachor models. Since the interfacial tensions were found to be independent of gas-oil ratio near equilibrium, interfacial tension measurements reported at a gas-oil ratio of 80/20 mole% gas and oil were used for modeling purpose in both the standard gas-oil systems.

The fluid phase compositions for gas-oil interfacial tension modeling were obtained by performing flash calculations with the commercial simulator Winprop (Computer Modeling Group Ltd., 2002) using the QNSS/Newton algorithm (Nghiem and Heidemann, 1982) and PR-EOS (Peng and Robinson, 1976). The measured densities of the fluid phases and the pure component Parachor values reported in literature (Quale, 1953; Fanchi, 1990; Ali, 1994; Schechter and Guo, 1998; Danesh, 1998) were used for interfacial tension calculations. The viscosities of the fluid phases needed for diffusivity calculations were computed using the Pederson's corresponding state model (Pederson and Fredenslund, 1987) within the commercial simulator, Winprop (Computer Modeling Group Ltd., 2002). The gas-oil interfacial tension modeling results obtained in both the standard gas-oil systems are summarized below.

❖ **n-Decane-CO_2 System at 100°F**

The comparison between the IFT predictions from the Parachor model and the experiments at various pressures in this gas-oil system at 100°F is given in Table 2.1. The results are also shown in Figure 2.1. As can be seen in Table 2.1 and Figure 2.1, a good match between the experiments and the model predictions is obtained with the Parachor model. This agrees well with the already published reports that the Parachor model predicts interfacial tensions reasonably well in binary mixtures (Weinaug and Katz, 1943; Fawcett, 1994). The good match of measured interfacial tensions with Parachor model indicates an exponent of zero in the proposed mechanistic Parachor model. The zero value for the exponent in the mechanistic model suggests equal proportions of vaporizing and condensing drive mechanisms in the combined vaporizing and condensing drive mechanism responsible for dynamic gas-oil miscibility development in this standard gas-oil system. This means that the amount of CO_2 dissolving in n-decane is about the same as the amount of n-decane vaporizing into CO_2 gas. The model interfacial tension predictions were fitted using the simple linear regression. The relation obtained is also indicated in Figure 2.1. A predicted VIT miscibility of 1121 psi was obtained by extrapolation of this relation to zero interfacial tension. This predicted miscibility deviates by only about 2.5% from the experimental VIT miscibility of 1150 psi obtained from the IFT measurements. This suggests that Parachor model is sufficient enough to accurately predict dynamic gas-oil miscibility in binary mixtures.

Table 2.1: Comparison of IFT Measurements with Parachor Model in n-Decane-CO_2 System at 100°F

Pressure (psi)	IFT (mN/m)	
	Experimental	Parachor Model
0	22.45	22.21
200	20.13	19.90
400	16.24	16.10
600	10.27	10.10
800	6.07	5.96
1000	3.34	3.21
1100	0.33	0.13

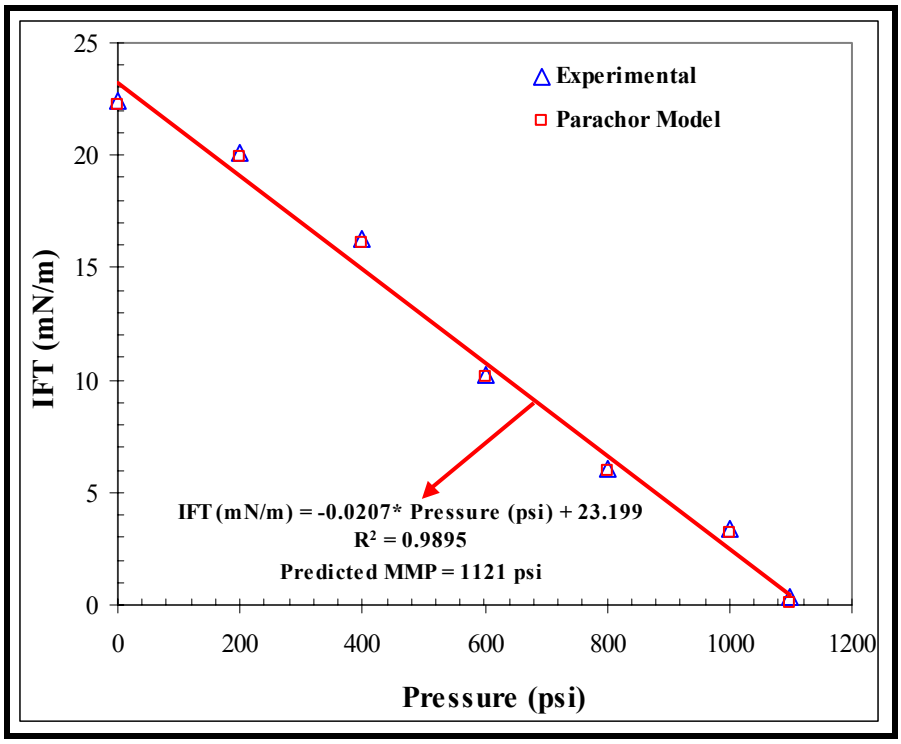

Figure 2.1: Comparison of IFT Measurements with Parachor Model in n-Decane-CO_2 System at 100°F

❖ **Live Decane-CO_2 System at 160°F**

The dynamic behavior of interfacial tensions measured in this gas-oil system has been discussed in the previous technical progress report (Report #15323R11, Oct. 2005). The comparison between interfacial tension predictions from the Parachor model and the dynamic interfacial tension measurements at various pressures is given in Table 2.2 and shown in Figure 2.2 for this standard gas-oil system at 160°F. As can be seen in Table 2.2 and Figure 2.2, the match between the experiments and the model predictions is not good and IFT under-predictions are obtained with the Parachor model. This was not the case in the binary system of n-decane-CO_2 discussed earlier. The disagreement between the experiments and the model predictions in gas-oil system indicates significant effects of interactions of one component with the others in terms of Parachor values in multicomponent hydrocarbon systems. This substantiates the poor performance of Parachor model for IFT predictions in multicomponent hydrocarbon systems, as reported by the other researchers also (Danesh et al., 1991; Fawcett, 1994). Hence, the mechanistic Parachor model has been applied to improve the IFT predictions in this gas-oil system by accounting for counter-directional mass transfer effects. Correction factors are used for the original Parachor model predictions to minimize the objective function, that is, the sum of weighted squared deviations between the original Parachor model predictions and the experimental IFT values. The mass transfer enhancement parameter (k), the

correction factor at which the objective function becomes the minimum was found to be 2.20.

Table 2.2: Comparison of IFT Measurements with Parachor and Mechanistic Parachor Models for Live Decane – CO_2 System at 160^{o}F

Pressure (psi)	IFT (mN/m)			Weighted Squared Dev.	
	Experimental	Parachor Model	Mechanistic Parachor Model	Parachor Model	Mechanistic Parachor Model
1100	4.061	2.394	5.267	0.1685	0.0881
1150	3.490	1.936	4.259	0.1982	0.0486
1200	2.712	1.526	3.357	0.1912	0.0566
1250	2.437	1.263	2.779	0.2321	0.0196
1300	2.041	1.056	2.323	0.2328	0.0192
1350	1.791	0.776	1.707	0.3211	0.0022
1400	1.373	0.614	1.351	0.3055	0.0003
1500	1.115	0.411	0.904	0.3986	0.0357
1550	0.887	0.300	0.660	0.4380	0.0655
1600	0.571	0.185	0.407	0.4572	0.0827
1650	0.441	0.138	0.304	0.4721	0.0971
1700	0.125	0.028	0.062	0.6016	0.2564
1750	0.044	0.014	0.031	0.4625	0.0877
			Objective Function	4.4794	0.8597

The diffusivities between the fluid phases at various pressures in this gas-oil system are given in Table 2.3. From Table 2.3, it can be seen that the average ratio of diffusivities between the fluids at all pressures is 3.0. From the mass transfer enhancement parameter and the average ratios of diffusivities between the fluid phases, the exponent (n) characterizing the governing mass transfer mechanism is found to be + 0.716. The positive sign of n indicates that vaporization of components from the oil into the gas phase is the controlling mass transfer mechanism in the combined vaporizing and condensing drive mechanism for attaining dynamic gas-oil miscibility in this standard gas-oil system. This can be attributed to the presence of significant amounts of lighter components (55 mole% methane and n-butane) in the live decane. The comparison between the mechanistic Parachor model IFT predictions and the experiments at various pressures is given in Table 2.2 and shown in Figure 2.2. As expected, a reasonably good match is obtained between the experiments and the mechanistic model predictions.

The modified version of the generalized regression model proposed for mechanistic model exponent prediction in crude oil-solvent systems (Report #15323R08, Jan. 2005) was utilized to determine the model exponent in this standard gas-oil system. This

regression model was originally developed for crude oil-solvent systems where solvent is the hydrocarbon gas mixture. However, in this standard gas-oil system, the solvent is the pure CO_2 gas. Therefore, the term representing condensing drive mechanism of intermediate to heavy components from solvent to oil in the regression model is not applicable and hence can be ignored. But the portion of the regression model representing the vaporizing drive mechanism holds true even for this case, as the lighter components (solute) vaporizing from oil into gas are almost similar in both the gas-oil systems. Furthermore, it is reasonable to add the component n-C_4 to the numerator in the term representing vaporizing drive mechanism, as its tendency will be primarily towards vaporization in the standard gas-oil system. With these assumptions, a mechanistic model exponent of 0.651 is obtained using the live decane composition in the generalized regression model for this standard gas-oil system. Thus, this exponent calculated using the compositional data in the regression model deviates by about 8.6% from the mechanistic model exponent of 0.716 obtained by using all the measured IFT experimental data.

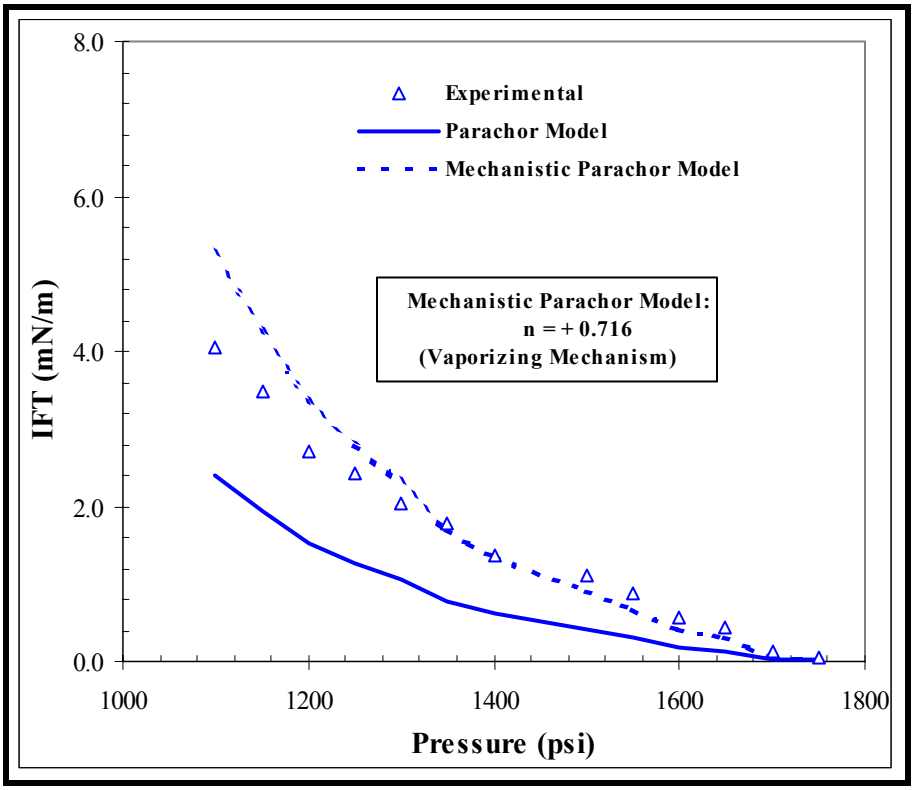

Figure 2.2: Comparison of IFT Measurements with Parachor and Mechanistic Parachor Models for Live Decane-CO_2 System at 160°F

Table 2.3: Diffusivities between Oil and Gas at Various Pressures in Live Decane – CO_2 System at 160°F

Pressure (psi)	$D_{oil-gas}$ (m^2/s)	$D_{gas-oil}$ (m^2/s)	$D_{oil-gas}/D_{gas-oil}$
1100	4.178E-08	1.251E-08	3.339
1150	4.100E-08	1.244E-08	3.295
1200	4.024E-08	1.238E-08	3.251
1250	3.952E-08	1.231E-08	3.210
1300	3.881E-08	1.224E-08	3.171
1350	3.797E-08	1.217E-08	3.119
1400	3.716E-08	1.211E-08	3.068
1500	3.521E-08	1.198E-08	2.940
1550	3.438E-08	1.192E-08	2.885
1600	3.333E-08	1.185E-08	2.812
1650	3.234E-08	1.180E-08	2.742
1700	3.141E-08	1.173E-08	2.677
1750	3.043E-08	1.167E-08	2.607
		Average =	3.009

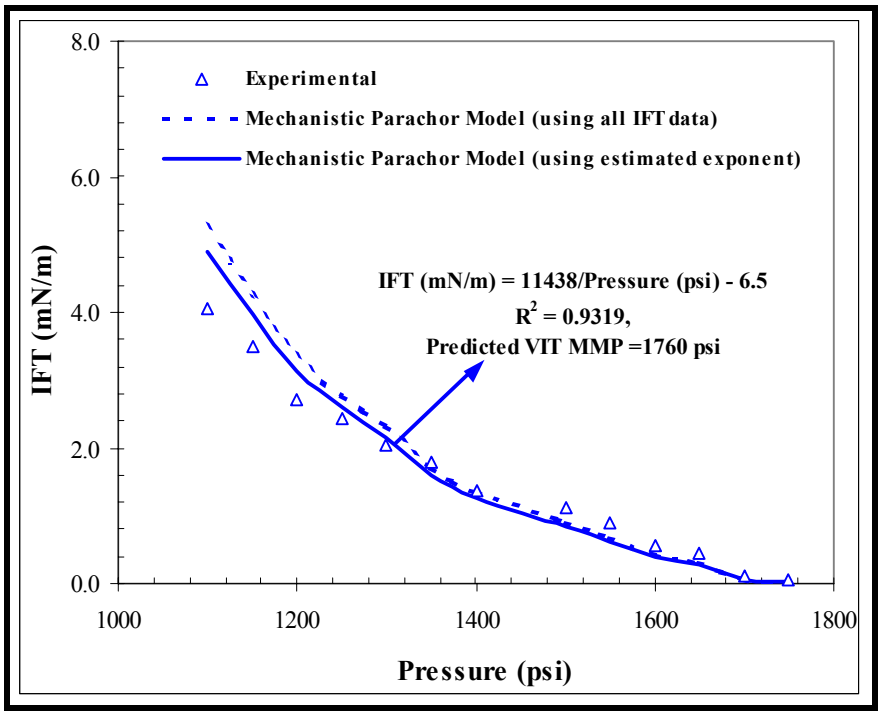

Figure 2.3: Comparison of IFT Measurements with Mechanistic Parachor Model of both the Exponents in Live Decane-CO_2 System at 160°F

The comparison between experiments and the predictions obtained using both the exponents in the mechanistic Parachor model for this standard gas-oil system are shown in Figure 2.3. From Figure 2.3, almost similar IFT predictions as well as good matches with IFT measurements can be seen from both the mechanistic Parachor models. This once again validates the use of a generalized regression model for the mechanistic model exponent prediction in crude oil-gas systems. The mechanistic model IFT predictions obtained using the exponent from the compositional data were then fitted against pressure using the hyperbolic function and the relationship obtained is shown in Figure 2.3. Extrapolation to zero interfacial tension gives a predicted VIT miscibility pressure of 1760 psi. This predicted VIT miscibility is identical to the experimentally measured VIT miscibility of 1760 psi. This indicates the applicability of mechanistic Parachor model to accurately predict dynamic gas-oil miscibility in multicomponent hydrocarbon mixtures.

2.2 Future Plans

Gas-oil interfacial tension measurements in selected crude oil-CO_2 gas system(s) are being planned for the next reporting quarter. The Parachor and mechanistic Parachor models will be utilized to model the gas-oil interfacial tensions measured as well as to infer the information on mass transfer mechanisms responsible for dynamic gas-oil miscibility development in crude oil-gas systems.

References

1. Ali, J.K.: "Predictions of Parachors and Petroleum Cuts and Pseudo Components," Fluid Phase Equilibria*,* 95 (1994) 383-398.
2. Computer Modeling Group Ltd., Winprop Phase Property Program, Calgary, Canada, 2002.
3. Danesh, A.S., Dandekar, A.Y., Todd, A.C. and Sarkar, R.: "A Modified Scaling Law and Parachor Method Approach for Improved Prediction of Interfacial Tension of Gas-Condensate Systems," paper SPE 22710 presented at the 66th SPE Annual Technical Conference and Exhibition, Dallas, TX, October 6-9, 1991.
4. Danesh, A., PVT and Phase Behavior of Petroleum Reservoir Fluids, Elsevier Science B.V., Amsterdam (1998).
5. Fanchi, J.R.: "Calculation of Parachors for Compositional Simulation: An Update," SPE Reservoir Engineering Journal, 5 (1990) 433-436.
6. Fawcett, M.J.: "Evaluation of Correlations and Parachors to Predict Low Interfacial Tension in Condensate Systems," paper SPE 28611 presented at the 69th SPE Annual Technical Conference and Exhibition, New Orleans, LA, September 25-28, 1994.
7. Nghiem, L.X. and Heidemann, R.A.: "General Acceleration Procedure for Multiphase Flash Calculations with Application to Oil-Gas-Water Systems," paper presented at

the 2nd European Symposium on Enhanced Oil Recovery, Paris, France, November 8-10, 1982.
8. Pederson, K.S. and Fredenslund, A.A.: "An Improved Corresponding States Model for Prediction of Oil and Gas Viscosities and Thermal Conductivities," Chem. Eng. Sci., 42 (1987) 182-186.
9. Peng, D.Y. and Robinson, D.B.: "A New Two-Constant Equation of State," Ind. Eng. Chem. Fundam., 15 (1976) 59-64.
10. Rao, D.N., Ayirala, S.C., Kulkarni, M.M. and Sharma, A.P.: "Development and Optimization of Gas-Assisted Gravity Drainage (GAGD) Process for Improved Light Oil Recovery," Annual Technical Progress Report to DOE, Report #15323R07, October 2004.
11. Rao, D.N., Ayirala, S.C., Kulkarni, M.M. and Sharma, A.P.: "Development and Optimization of Gas-Assisted Gravity Drainage (GAGD) Process for Improved Light Oil Recovery," Quarterly Technical Progress Report to DOE, Report #15323R08, January 2005.
12. Rao, D.N., Ayirala, S.C., Kulkarni, M.M. and Sharma, A.P.: "Development and Optimization of Gas-Assisted Gravity Drainage (GAGD) Process for Improved Light Oil Recovery," Annual Technical Progress Report to DOE, Report #15323R11, October 2005.
13. Quale, O.R.: "The Parachors of Organic Compounds," Chem. Review, 53 (1953) 439-586.
14. Schechter, D.S. and Guo, B.: "Parachors Based on Modern Physics and Their Uses in IFT Prediction of Reservoir Fluids," SPE Reservoir Evaluation & Engineering Journal, 1 (1998) 207-217.
15. Weinaug, C.F. and Katz, D.L.: "Surface Tensions of Methane-Propane Mixtures," Industrial Engineering Chemistry, 35 (1943) 239-246.

3. Determination of Multiphase Displacement Characteristics In Reservoir Rocks

This section of the progress report includes the continued research work aimed at evaluating the multiphase displacement characteristics of water-alternating-gas and gas assisted gravity stable gas injection processes in Berea and reservoir rocks. In the previous reports to the DOE (15323R07, Oct 2004; 15323R08, Jan 2005; 15323R09, Apr 2005; 15323R10, July 2005 and 154323, Oct 2005), the 1-D experimental results from dimensionally scaled GAGD and WAG corefloods were reported. Section 1 reports the experimental results from 2-D physical model experiments. This section attempts to extend this study to 3-D (4-phase) flow through porous media and evaluate the performance of these processes using reservoir simulation.

3.1 Preliminary Reservoir Simulation Study of WAG and GAGD Processes using IMEX®

To study the effects of the various design parameters discussed above, a full-field statistical reservoir model 'PETE-7231-Field' was developed using a commercial simulator (CMG IMEX® with pseudo-miscible option without the chase gas option). IMEX® is CMG's implicit explicit black oil simulator, and can be used to model the flow of three phase fluids in gas, gas-water, oil-water, and oil-water-gas reservoirs. It models in one, two, or three dimensions; including complex heterogeneous faulted structures.

A 3500 (25 x 35 x 4) grid block model was developed for the hypothetical field. The contour map of the statistical reservoir is shown as Figure 3.1. The mathematical model consisted of four-phase (O/W/G/S) 'pseudomiscible' type fluid flow, and field was assumed to be developed using 18 wells and 5 constraint types.

3.1.1 History of the Hypothetical Statistical Reservoir

The hypothetical reservoir was discovered by the wildcat exploratory well E001 in 1990. The seismic analysis of the reservoir suggested the location of this wildcat in the thickest portion of the reservoir and encountered 556 ft sand thickness. The reservoir was composed of two 'mounds' of thick sands joint together to form a reef type of reservoir, with the thickness of the reservoir decreasing towards the edges to zero ft. The 3-D view of the reservoir is shown as Figure 3.2. Seven developmental production wells P001 through P007 were drilled and the entire field put on production on Jan 01, 1991. The simulation runs were conducted for about 100 years to check for the ultimate recoveries. Economic limits were not set to ensure accuracy in estimates of ultimate 'volumetric' recoveries from this field.

3.1.2 Reservoir Petrophysical Properties

The average reservoir porosity was estimated to be 19%. The reservoir porosities were generated using a statistical random number generator function. The permeabilities were calculated using the porosity data using a formula function to make the reservoir properties purely statistical. Average I and J directional perms were estimated to be 230 mD, and the ratio of vertical and horizontal permeabilities (K_V/K_H) was 0.5.

3.1.3 Reservoir Fluid Properties

The reservoir oil gravity was 35^o API with the solution gas gravity of 0.65. The associated reservoir water has a salinity of 5000-ppm. The PVT properties were calculated from correlations using the reference reservoir pressure of 4000 psia, and the initial GOR (Gas-Oil-Ratio) as 1000 SCF/STB.

3.1.4 Reservoir Rock-Fluid Properties

In reservoir simulation, the combined effects of wettability, interfacial tension, fluid saturations and flow dispersion are generally lumped into a single parameter: relative permeability. Relative permeability can be calculated from empirical correlations or can be experimentally determined. The reservoir-rock permeabilities for this model were calculated from correlations using the end point values of the laboratory floods. Critical gas saturation was set at 0.05 and all Corey exponents as 2.0. Three phase relative permeability values were calculated using the Stone-II model. The relative permeability curves for oil-water and liquid-gas have been included as Figure 3.3.

All the oil / gas / solvent properties are summarized in Figures 3.4 and 3.5. Hydrocarbon fluid properties summarized are solution GOR (R_S), oil FVF (B_O), gas compressibility factor (Z_G), gas FVF (B_G), oil and gas viscosity (VisG & VisO) parameters. Three-phase oil relative permeability calculated using the Stone II model, is also included. Solvent properties have been summarized in solvent compressibility factor (Z_S), solvent viscosity (VisS), solvent expansion factor (E_S) and mixing parameter between oil and solvent responsible for miscibility (Omega_OS).

3.1.5 Reservoir Model Assumptions

The assumptions made for the initialization and execution of the model are summarized below.

- EOR is applied as tertiary process
- Secondary recovery process is waterflood.
- Reservoir is purely volumetric and undersaturated without any aquifer support.
- No capillary pressure.
- Injected gas is carbon-dioxide (CO_2) without any chase gas flooding.

- Injection pattern is normal 5-spot.
- Leas and Rappaport[1] and Rutherford[2] stability criterion applicable to horizontal and vertical immiscible floods respectively.
- Economic production rates for primary and secondary (Waterflood) processes are 1000 BBL/D and 1500 BBL/D respectively; with no set economic limits for tertiary production.

3.1.6 Model Initialization Results

The results (Table 3.1) of the full field model initialization are partially summarized below:

- Total PV: 678451 MSTB.
- Hydrocarbon PV: 542610 MSTB.
- Original Oil in Place (OOIP): 368455 MSTB.
- Original Gas in Place (OGIP): 368173 MMSCF.
- Original Water in Place (OWIP): 136201 MSTB.
- Average reservoir pressure: 4038 psia.
- Average saturations were estimated as:
    - Oil: 79.98 %
    - Gas: 100E-06 %
    - Water: 20.02 %

3.1.7 Base Runs

The hypothetical 'PETE-7231-Field' was put on production on Jan 01, 1991. The maximum primary production rate was set to 50,000 BBL/D. However, steep decline in reservoir pressure and production rates were observed in Jan 1995. Hence, ten developmental wells were drilled to efficiently drain the reservoir. The plan-view of the reservoir with all drilled wells is shown in Figure 3.6. Further, a 30-year reservoir pressure maintenance program by waterflooding was planned and implemented in Jan 1998. Eight developmental wells were converted to water-injectors in a normal five-spot injection pattern. Leas and Rappaport[1] criterion was used to ensure stability of the flood. However, high increases in water-cut were observed towards the end of the flood (> 90%) and oil productions fell below economic limit; hence and a tertiary flood is planned in Jan 2027. The objective of this simulation study is to compare & determine the 'best' tertiary flood pattern for this reservoir using CO_2 gas based on higher recoveries predicted by the laboratory tests and availability. The processes evaluated were:

- Continuous CO_2 Injection (horizontal flood).
- Water-Alternate-Gas Injection (horizontal flood).
- Gravity Stable gas injection.

3.1.8 Sensitivity Runs

Reservoir heterogeneity characterization is one of the most difficult tasks required for reservoir simulation. Heterogeneity is of high importance for displacement processes because it dictates the reservoir fluid mechanics in the reservoir. Hence to isolate and understand the effects of heterogeneity, two models were studied: One homogeneous and other heterogeneous – keeping all other reservoir parameters constant. Similar sensitivity runs were conducted for both the models. The runs conducted after waterflooding at 4900 BBL/D rates are:

- Cumulative WAG injection rates kept constant at 0.05 PV/year (From CMG).
- Continuous gas flood:
    - Effect of flood rates (0.05, 0.10, 0.20 PV/year)
- WAG Flood:
    - Effect of slug size:
        Equal slug size (0.2 PV)
    - Twice slug size (0.4 PV)
        Quadrupled slug size (0.6 PV)
    - Effect of WAG ratio:
        Equal (1:1)
        Twice water slug (2:1)
        Quadrupled water slug (4:1)
- Gravity drainage flood rates:
    - Injection rates equal to 1:1 WAG CO_2 injection rates.
    - Horizontal well lengths: 4500 ft & 2500 ft.

3.2 Simulation Results

3.2.1 Homogeneous Reservoir

Tertiary flood was planned on Jan 2027 due to high water cuts predicted by reservoir simulation. Simulations showed high residual oil saturations (~ 40%) in the thickest part of the reservoir as shown in Figure 3.7. The oil potential is depicted in Figure 3.8. Hence a 5-spot injection pattern was chosen to confine the oil and produce it.

Plain CO_2 injection and WAG were evaluated for this homogeneous reservoir. Flooding rates were limited to the stable regions, using the Leas and Rappaport[1] criterion. The effect of WAG ratios was negligible on oil production; hence it was concluded that the WAG ratio was not a parameter in this reservoir. The WAG runs were evaluated with slug size ratios varying from 1:1 to 4:1 and each of the ratios were tested for varying slug sizes from 4:1 to 1:4 (Water-to-Gas slug sizes).

- **Effect of WAG Slug Size**

The sensitivity runs were conducted for 1:1, 2:1 and 4:1 water-to-gas slug size ratios. The incremental production by increasing the slug size was not very much higher than the oil

production for 1:1 ratio. Noticeable increases in oil production were only observed at very high injection rates. Similar productions are observed for 1:1 and 2:1 slug sizes as shown in Figure 3.9; hence the economics suggest the use of 2:1 or 0.4 PV water and 0.2 PV gas slug size for the implementation of the WAG in this reservoir.

- **Effect of CO_2 Injection Rates**

The plain CO_2 injection was evaluated by choosing the injection rates as equal, twice, 4-times and 8-times the CO_2 injection rates (upper limit was the Leas and Rappaport[1] maximum stable injection rate) in the gas half cycle of the WAG flood. The reservoir shows monotonous increases with cumulative oil productions with the injection rates (Figure 3.10).

3.2.2 Heterogeneous Reservoir

Heterogeneity was introduced in the homogeneous reservoir previously considered by varying the porosity and calculating I and J directional permeability based on porosity value of the grid block / layer. The K_V/K_H ratio was fixed at 0.5. This reservoir was simulated similar to the homogeneous case; and the tertiary flood was planned on Jan 2027 due to high water cuts. This is shown in Figure 3.11(a).

The simulations showed high residual oil saturations (~ 45%) in the thickest part of the reservoir. Thus, the heterogeneity effects retained about 5% of the OOIP after a secondary waterflood. Based on the oil potential, as depicted in Figure 3.11(b), a 5-spot injection pattern was chosen to confine the oil and produce it.

Plain CO_2 injection, WAG and gravity stable gas injection were also evaluated for this reservoir. Flooding rates were limited to the stable regions, using the Leas and Rappaport[1] criterion.

- **Effect of WAG Ratio**

As against the homogeneous case, the WAG ratio played a significant role in this heterogeneous reservoir (Figure 3.12). Although the effect of WAG ratio on incremental oil production is negligible; the 2:1 WAG produces as much as the 1:1 WAG but in very less time. Hence, from economics point of view, the 2:1 WAG is most suited for this water-wet heterogeneous reservoir.

- **Effect of WAG Slug Size**

The WAG runs were further evaluated with slug size ratios varying from 1:1 to 4:1 and each of the ratios were tested for varying slug sizes from 4:1 to 1:4 (Water – to – Gas slug sizes) to arrive at the best slug size.

Increase in the CO_2 slug size did not help optimize the WAG process; instead, early breakthrough and bypassing resulted in CO_2 doing little good. Comparable oil productions were observed for 1:1 and 2:1 slug size WAG floods. However, higher recovery rates and lower cumulative CO_2 injection helps the 2:1 slug size WAG process be ideal for this reservoir, whose production plots are shown in Figure 3.13.

- **Effect of CO_2 Injection Rates**

The plain CO_2 injection was evaluated by choosing the injection rates as equal, twice, 4-times and 8-times the CO_2 injection rates in the gas half cycle of the WAG flood. The reservoir shows comparable cumulative oil productions for 0:0.5 and 0:1 CO_2 injection rates. However, as the injection rates are increased further (0:2 & 0:4), the early breakthrough and bypassing problems are observed. Hence, for better recovery and high-sustained production rates 0:1 CO_2 injection would be optimum. The production plots of which are shown in Figure 3.14.

- **Gravity Stable (GAGD) Flood**

Simulation runs to study the effects of gravity stable (GAGD) flooding were conducted for this heterogeneous reservoir. The plain CO_2 gas was injected in a 5-spot pattern (similar to WAG and plain CO_2), with wells completed only in the top layer, at injection rates equal to 1:1 WAG (or 0:0.5 plain CO_2). All the other wells were plugged to simulate identical reservoir conditions to WAG and plain CO_2, and to facilitate comparison between the processes. This gravity stable injection called for drilling three horizontal producers at the bottom of the payzone; hence it was necessary to determine the production from these horizontal wells to evaluate incremental productions due to gravity stable gas injection. Simulation runs were conducted with and without injection gas to determine the influence of the horizontal producers.

Two lengths of horizontal wells were evaluated, 4500 ft (encompassing the whole bottom portion of the reservoir) and 2500 ft (practical and common lengths of horizontal wells drilled in United States). The simulations showed unappreciable difference in production rates and incremental oil production. The results of which are included in Figure 3.15. Hence, it would not be unreasonable to assume that all the incremental oil over the waterflood is due to gravity drainage.

The simulation runs suggest early response for 4500' well; however, this effect is quickly nullified by the better drainage characteristics of the 2500' well, and ultimate production are not highly different. Hence, the incremental cost involved in drilling longer horizontal wells is not advised. This can be clearly observed from the simulation results in Figure 3.16. Furthermore, there is significant delay in the breakthrough of gas through the horizontal well. The gas saturations in each of the four layers are shown in Figure 3.17 for 100 years of gravity drainage.

3.3 Simulation Results

The 2:1 WAG is the optimal process for the homogeneous reservoir. However, there is a choice between 2:1 WAG, 0:1 plain CO_2 injection, and gravity stable gas injection (GAGD) for the heterogeneous reservoir. For the execution of the WAG and plain CO_2 injection, there is no additional need for drilling wells, whereas for the gravity stable gas

injection three new horizontal producers need be drilled. The economics of the processes will dictate the 'best' EOR process for this reservoir.

However, some interesting conclusions can be drawn from evaluation of production rates and some simple economic calculations. Figures 3.18 and 3.19 show the comparative plots of the three processes for the heterogeneous reservoir.

The oil production from the gravity drainage (GAGD) is the highest followed by plain CO_2 injection. WAG process yields lower recoveries but the CO_2 consumption is the lowest and better utilization of the CO_2 is achieved in the WAG process. Hence economics were considered. Table 3.2 gives the comparative evaluation of the processes. It is important to note that the cost of drilling horizontal wells is not considered in the following economic analysis. The cost of drilling these wells would ultimately influence the overall economics.

3.3.1 Preliminary Observations

The major preliminary observations from this study are:

- Homogeneous reservoirs show monotonously increases in oil recoveries with increasing CO_2 cumulative injection.
- Homogeneous reservoirs do not show drastic responses to increases in WAG ratio or slug sizes.
- Reservoir heterogeneity seemed to affect primary and secondary production processes more than the tertiary processes (Figure 3.20).
- Plain CO_2 yields better recoveries than WAG for water-wet reservoirs. The model results agree well with the experimental conclusions of Jensen et al[3].
- Optimum slug size for WAG injections is 0.4 PV to 0.2 PV. Simulation results exactly agree with literature[3][4].
- Model further showed that good recoveries could be achieved with WAG with much lower cumulative CO_2 injection requirements.
- Gravity stable injection could be the optimum EOR alternative however, cost of drilling the horizontal producers need to be economically evaluated.

3.3.2 Relevance of Reservoir Simulation to EOR

This study shows the practical implications of reservoir simulators for designing EOR floods. Although, the execution of these simulators requires expertise, simplification and user-friendly programs are being developed and are available. Constant upgrades and incorporation of new models to accurately model flow and phase behavior will help reservoir simulation be a very important tool for EOR design. The relevance is summarized as,

- Capability to model reservoir heterogeneity, which could dictate an EOR process

successful or otherwise.

- Ease in handling reservoir data uncertainties and perform sensitivity analysis to correct and upgrade reservoir properties.
- Ease in quick incorporation of new available data.
- Use in design stages where data is limited and uncertainties are high.
- Use in evaluation of new processes yet to be tried on field scale and predict reservoir behavior with reasonable accuracy.

3.4 Future Work

1. Use of volume based WAG instead of time based.
2. Development of a similar fully compositional model to validate and extrapolate the results of this study.
3. Development of an accurate model for characterization of the drainage and imbibition cycles that are an indispensable part of the WAG process.
4. Improvements in characterization of the reservoir wettability for direct use in reservoir simulators.
5. Need for pilot testing.

References

1. Rappaport, L. A., Leas, W. J., "Properties of Linear Waterfloods", Trans. AIME, (1953) 198, pp. 139
2. Stalkup Jr., F. I., "Miscible Displacement", Monograph Volume 8, Society of Petroleum Engineers, Henry L Doherty Series, 1985
3. Christensen, J. R., Stenby, E. H., Skauge, A., "Review of the WAG field experience", SPE 71203, revised paper 39883, presented at the 1998 SPE International petroleum conference and exhibition of Mexico, Villhermosa, March 3-5, 1998
4. Jackson, D. D., Andrews, G. L., Claridge, E. L., "Optimum WAG ratio Vs Rock wettability in CO_2 flooding", SPE 14303, presented at 60^{th} Annual technical conference and exhibition of the Society of Petroleum engineers held in Las Vegas, NV, Sept 22-25,1985.

Table 3.1: Summary of important simulation results

(a) Model Results

OOIP	368455 MSTB
OGIP	368173 MMCF (Dissolved)
OWIP	136201 MSTB

(b) Homogeneous 'PETE-7231-Field'

2:1 WAG optimal WAG	Recovery is 40.17 %
0:2 plain CO_2 injecn next best	Recovery is 47.17 %

(c) Heterogeneous 'PETE-7231-Field'

2:1 WAG optimal WAG	Recovery is 39.08 %
0:1 plain CO_2 injecn	Recovery is 47.5 % (most economical)
No significant effect of WAG ratio	
2500' Gravity drainage	51.87% (Economics strongly dependant on horiz well cost)

Table 3.2: Comparison of productions and economics for the tertiary process

	Heterogeneous				**Homogeneous**
	GAGD	**0:1 CO2**	**2:1WAG**	**WF**	**2:1WAG(H)**
Oil (Bbl)	1.91E+08	1.75E+08	1.45E+08	1.36E+08	1.48E+08
Oil Revenue ($)	1.38E+09	9.80E+08	2.24E+08	0.00E+00	1.66E+08
Gas (SCF)	3.28E+11	3.24E+11	3.15E+11	3.06E+11	3.12E+11
Gas Revenue ($)	8.80E+04	7.20E+04	3.67E+04	0.00E+00	3.28E+04
Hydrocarbon Revenue ($)	1.38E+09	9.80E+08	2.24E+08	0.00E+00	1.66E+08
CO_2 (SCF)	1.89E+10	1.87E+10	3.06E+09	0.00E+00	2.39E+11
CO_2 Expense ($)	1.14E+04	1.12E+04	1.83E+03	0.00E+00	1.43E+05
Profit ($)	1.38E+09	9.80E+08	2.24E+08	0.00E+00	1.66E+08

(Assumed Oil: $25/bbl; Gas $4/MCF & CO_2 $0.60/MCF)

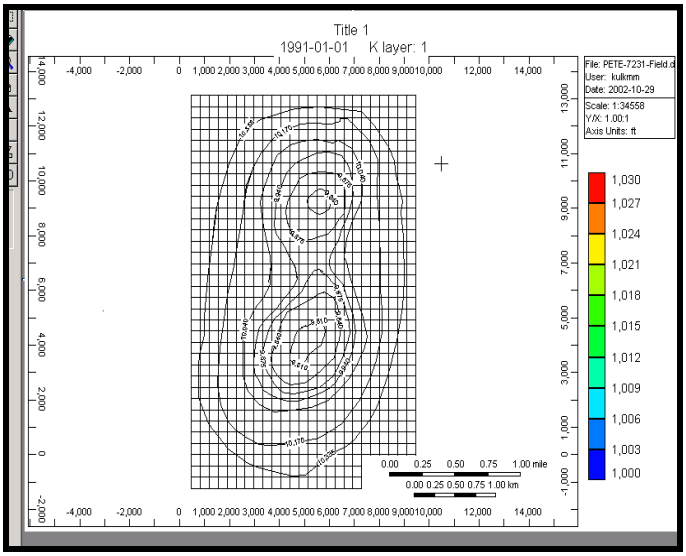

Figure 3.1: Contour Map of the 'PETE-7231-Field'

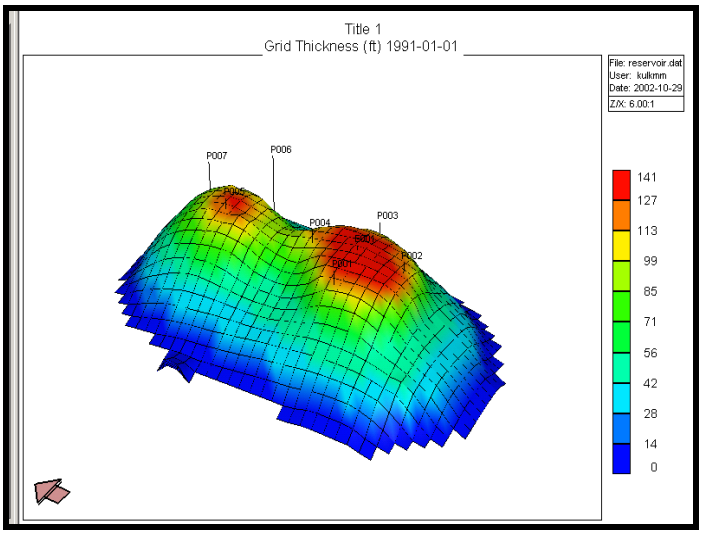

Figure 3.2: 3-D reservoir map of the 'PETE-7231-Field'

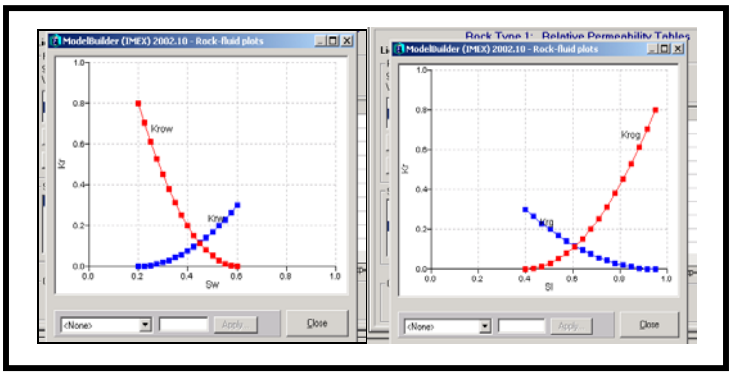

Figure 3.3: O-W & L-G Relative permeability characteristics

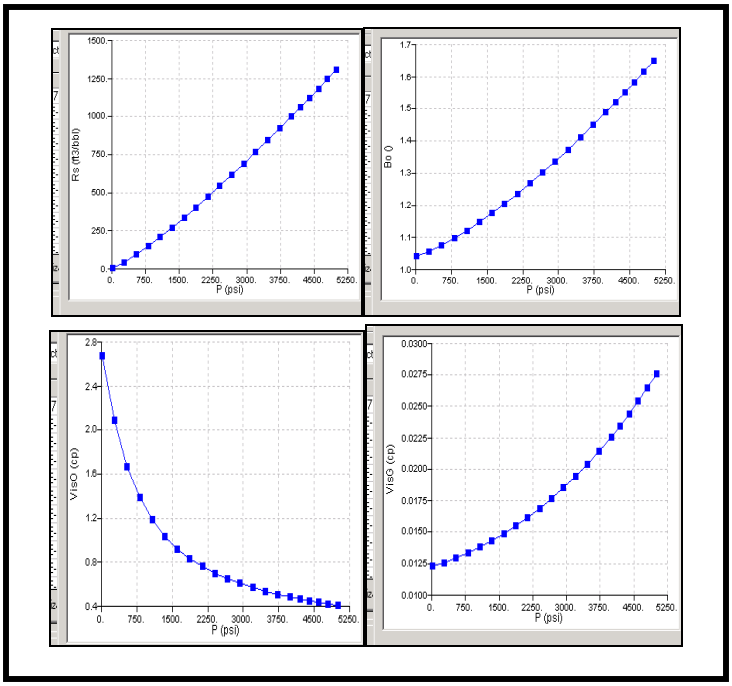

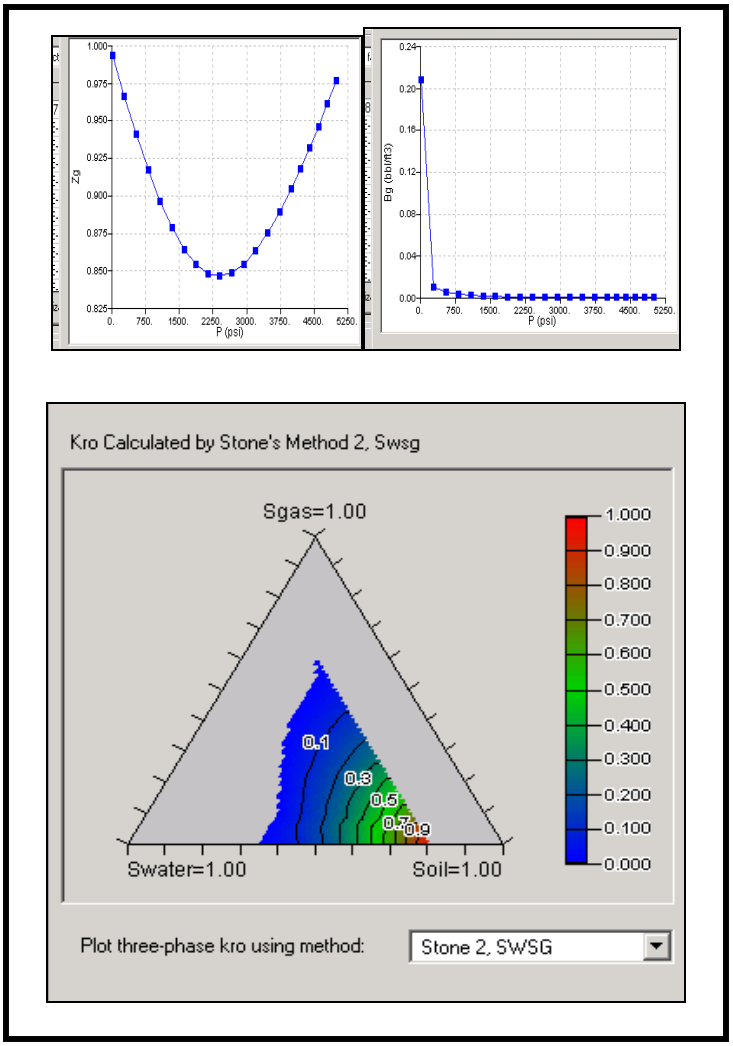

Figure 3.4: Hydrocarbon reservoir fluid phase properties

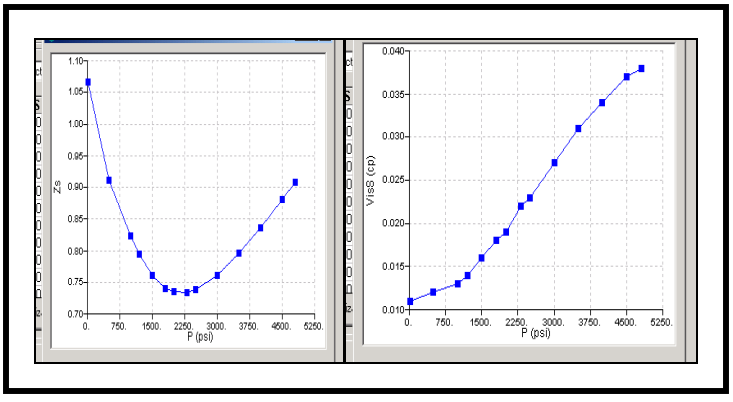

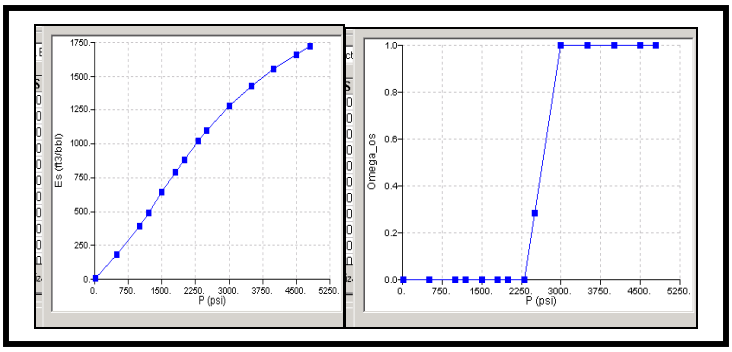

Figure 3.5: Solvent (CO_2) fluid phase properties

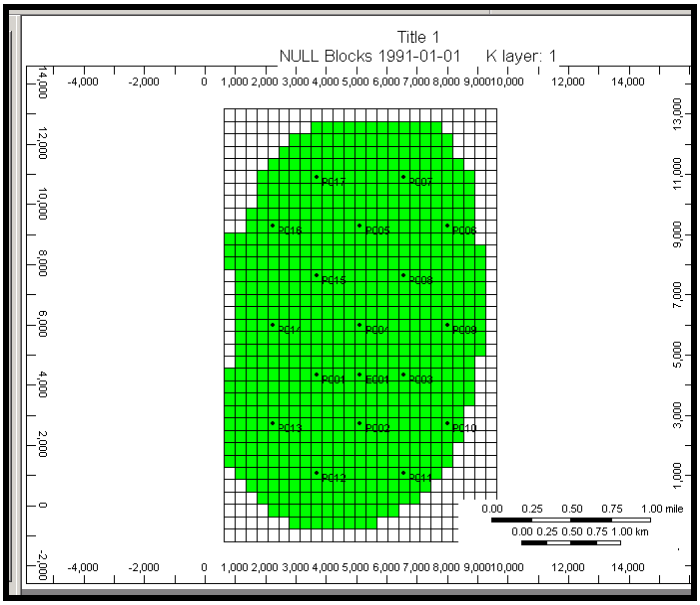

Figure 3.6: Well placement pattern in 'PETE-7231-Field'

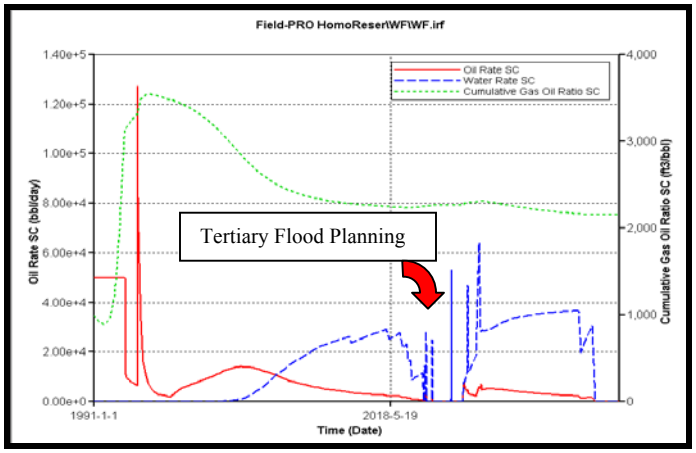

Figure 3.7: Production patterns in homogeneous reservoir for the 'PETE-7231-Field'

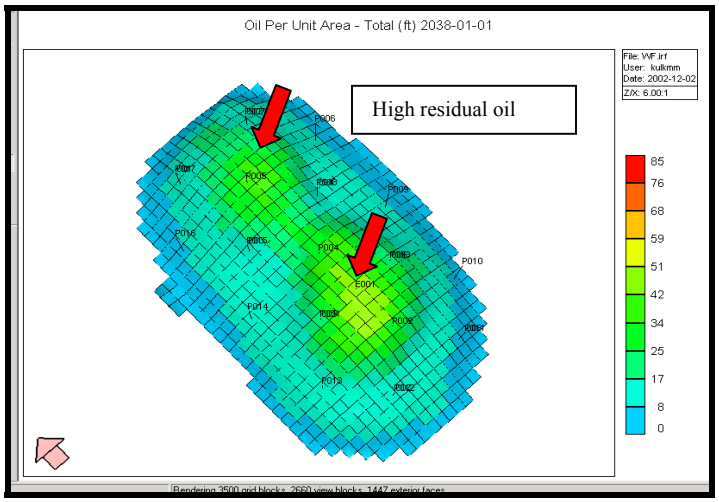

Figure 3.8: Residual oil saturation after a secondary WF for homogeneous reservoir for the 'PETE-7231-Field'

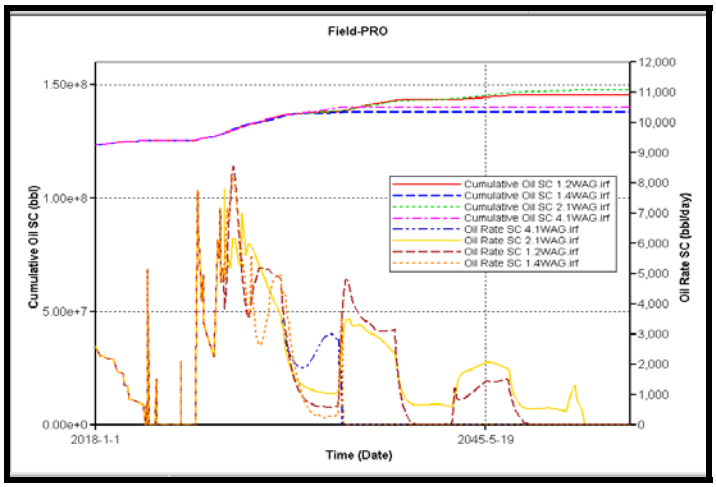

Figure 3.9: Effect of slug size on tertiary oil rates and cumulative oil production for homogeneous reservoir 'PETE-7231-Field'

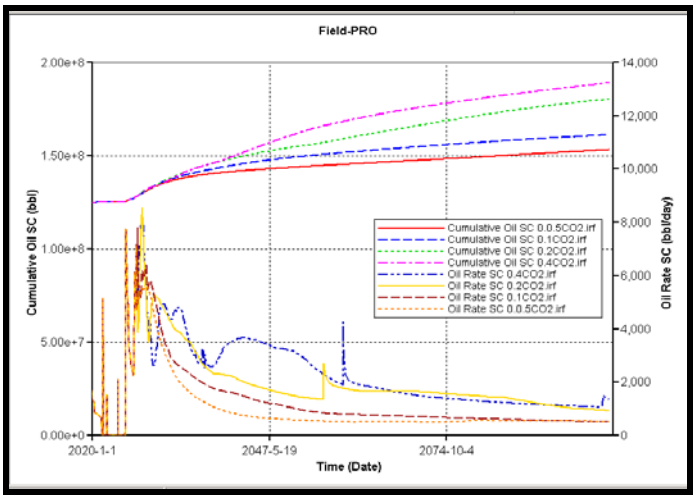

Figure 3.10: Effect of CO_2 injection rates on tertiary oil rates and cumulative oil production for homogeneous reservoir 'PETE-7231-Field'

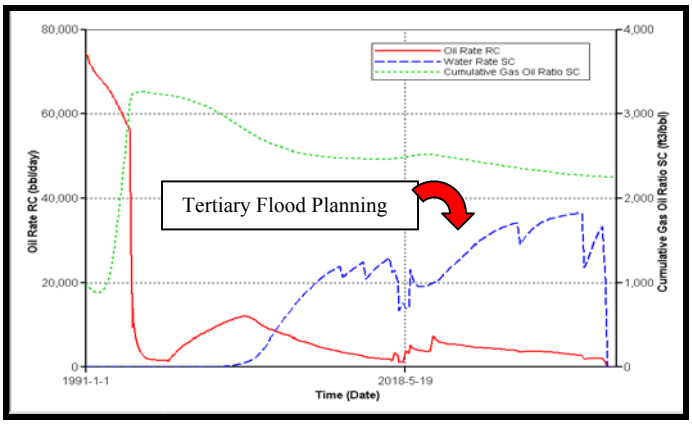

Figure 3.11(a): Production patterns in heterogeneous reservoir for 'PETE-7231-Field'

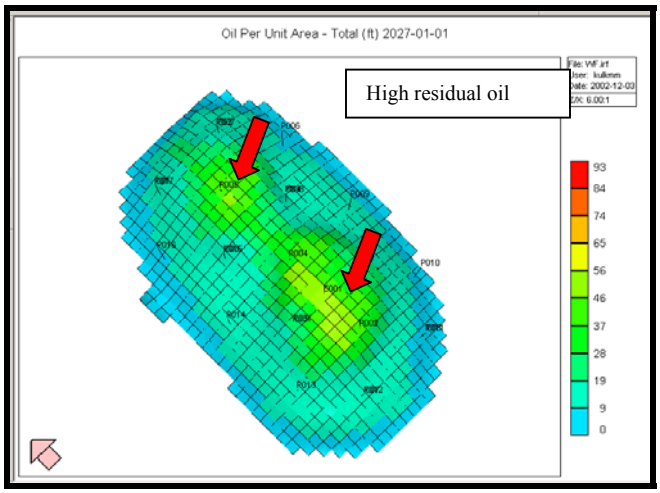

Figure 3.11(b): Residual oil saturation after a secondary WF for heterogeneous reservoir for the 'PETE-7231-Field'

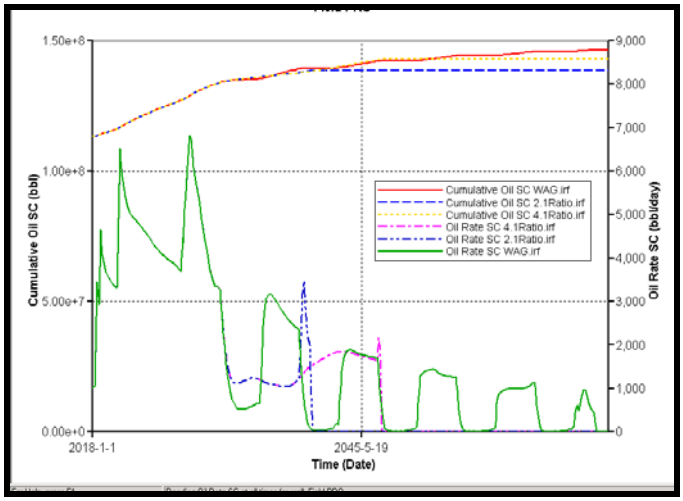

Figure 3.12: Effect of WAG ratio on tertiary oil rates and cumulative oil production for heterogeneous reservoir 'PETE-7231-Field'

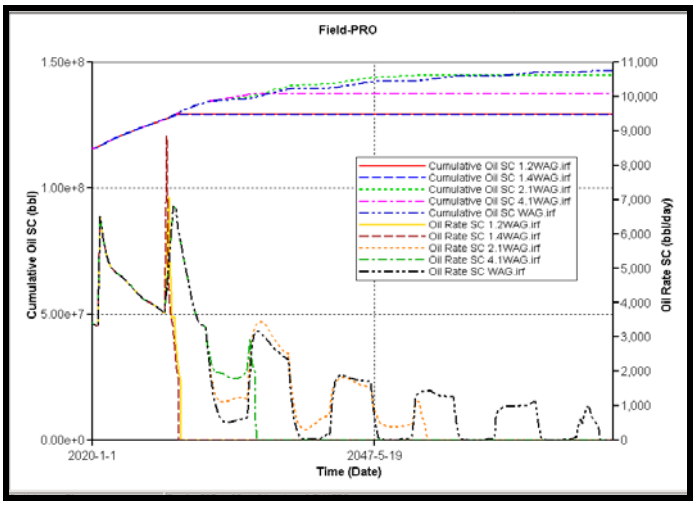

Figure 3.13: Effect of slug size (WAG) ratio on tertiary oil rates and cumulative oil production for heterogeneous reservoir 'PETE-7231-Field'

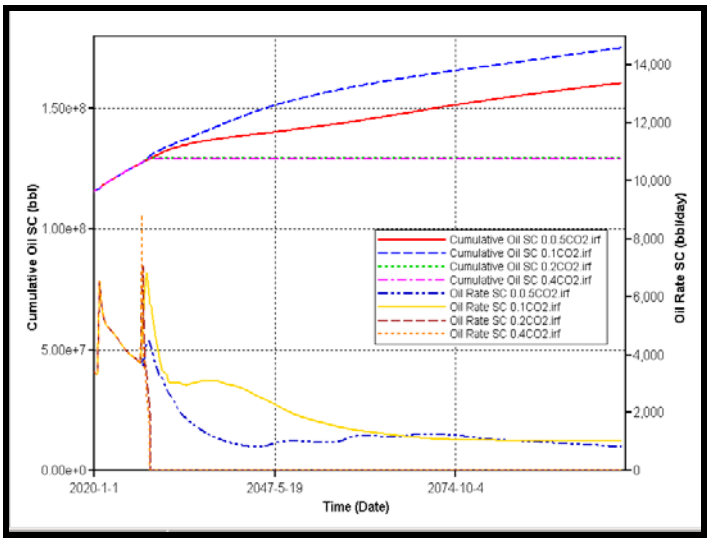

Figure 3.14: Effect of CO_2 injection rate on tertiary and cumulative oil for heterogeneous reservoir 'PETE-7231-Field'

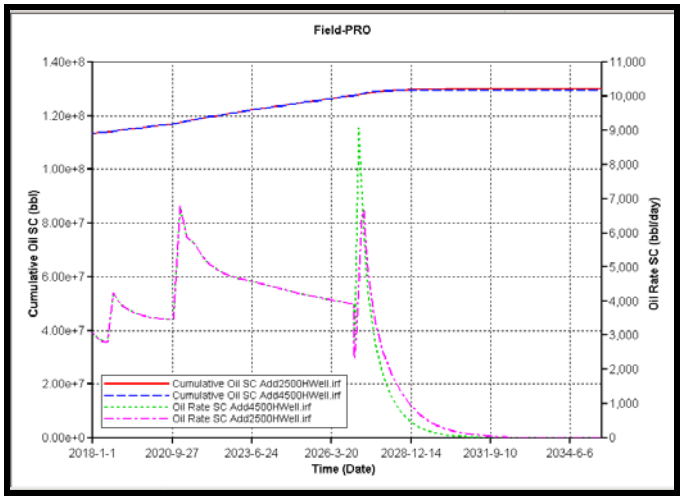

Figure 3.15: Effect of horizontal producers on tertiary and cumulative oil for heterogeneous reservoir 'PETE-7231-Field'

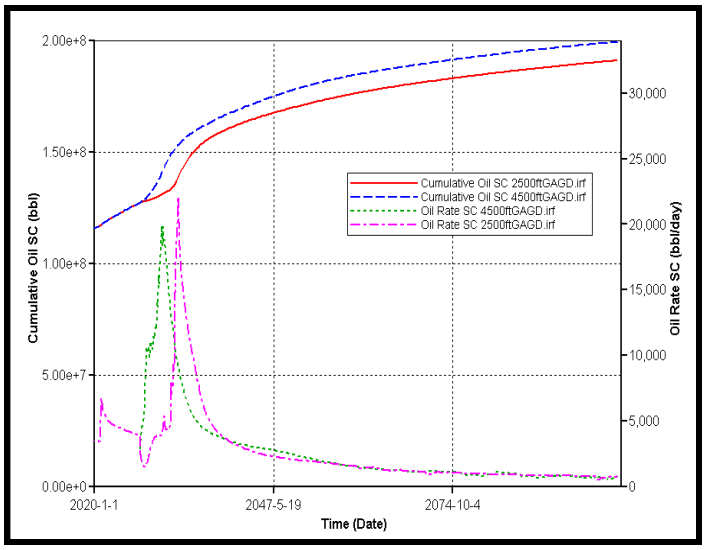

Figure 3.16: Effect of gravity drainage on tertiary and cumulative oil for heterogeneous reservoir 'PETE-7231-Field'

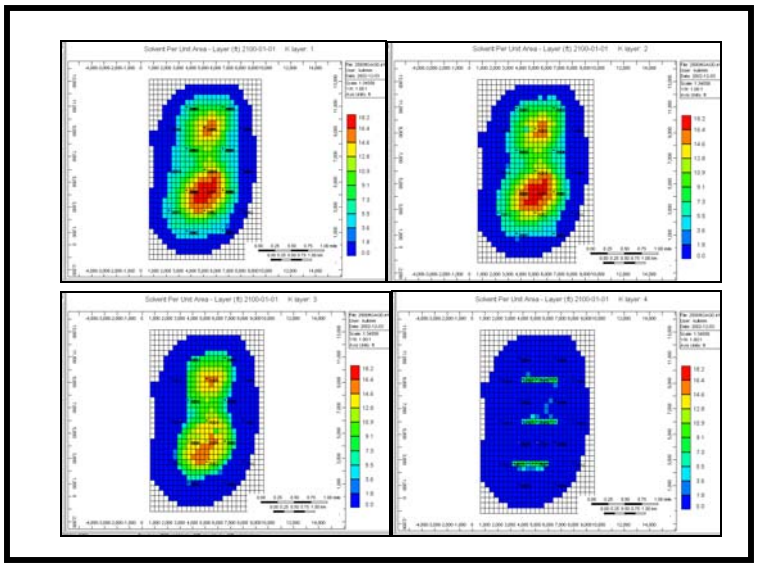

Figure 3.17: Delayed breakthrough and formation of 'chamber' of solvent due to injection in gravity stable mode for heterogeneous reservoir 'PETE-7231-Field'

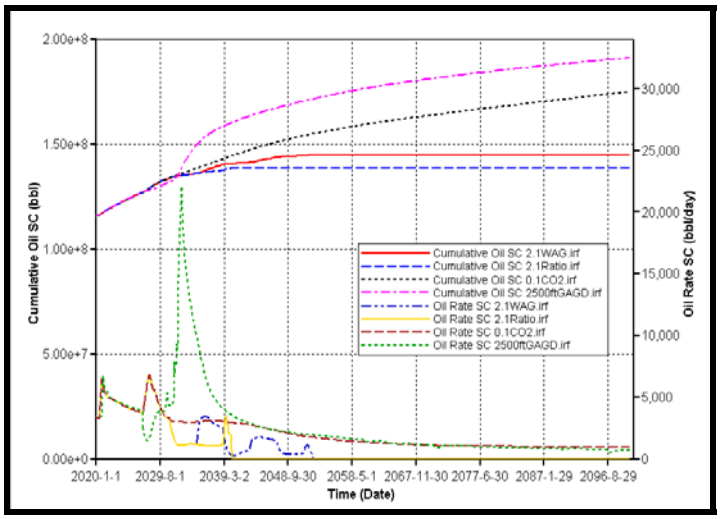

Figure 3.18: Comparison of possible tertiary EOR processes for heterogeneous reservoir 'PETE-7231-Field'

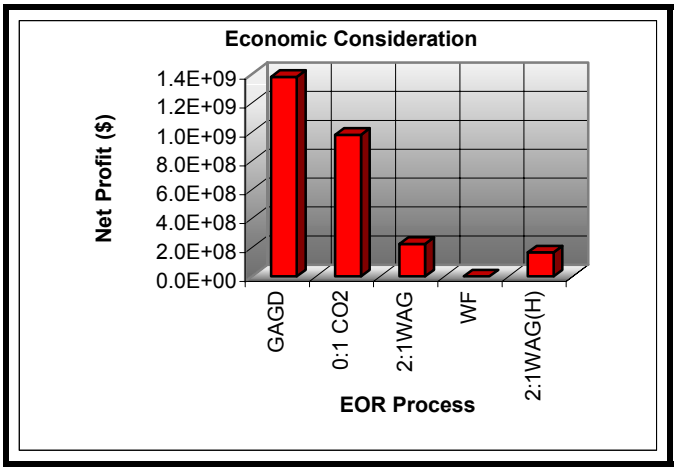

Figure 3.19: Economic comparisons between the EOR processes considered. (H) Symbolizes homogeneous reservoir

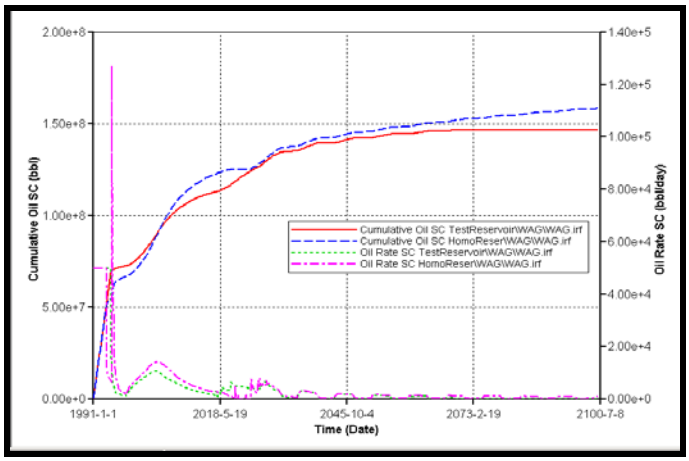

Figure 3.20: Effects of rock heterogeneity on WAG

4. Technology Transfer Efforts

Numerous technology transfer efforts were carried out by the LSU-EOR Research Group during this reporting quarter Oct – Dec 2005. The research efforts during this reporting period resulted in one technical paper, one journal publication; three pending abstracts for SCA 2006 Annual Conference and an invitation to present at the Independents' Day session at the IOR Symposium 2006.

4.1 Technical Papers Prepared

1. Ayirala, S. C., and Rao, D. N., "Comparative Evaluation of a New MMP Determination Technique", SPE 99606, 15th SPE Improved Oil Recovery Symposium, Tulsa, OK, Apr 22-26, 2006
2. Ayirala, S. C., Xu, W., and Rao, D. N., "Interfacial Behavior of Complex Hydrocarbon Fluids at Elevated Pressures and Temperatures", the Canadian Journal of Chemical Engineering, Vol. 84, February 2006.
3. Rao, D. N., "Gas Assisted (CO_2) Gravity Drainage IOR; The Process and a Louisiana Field Project", Invited talk at the Independents Day @ IOR 2006, Tulsa, OK, Apr 25, 2006.